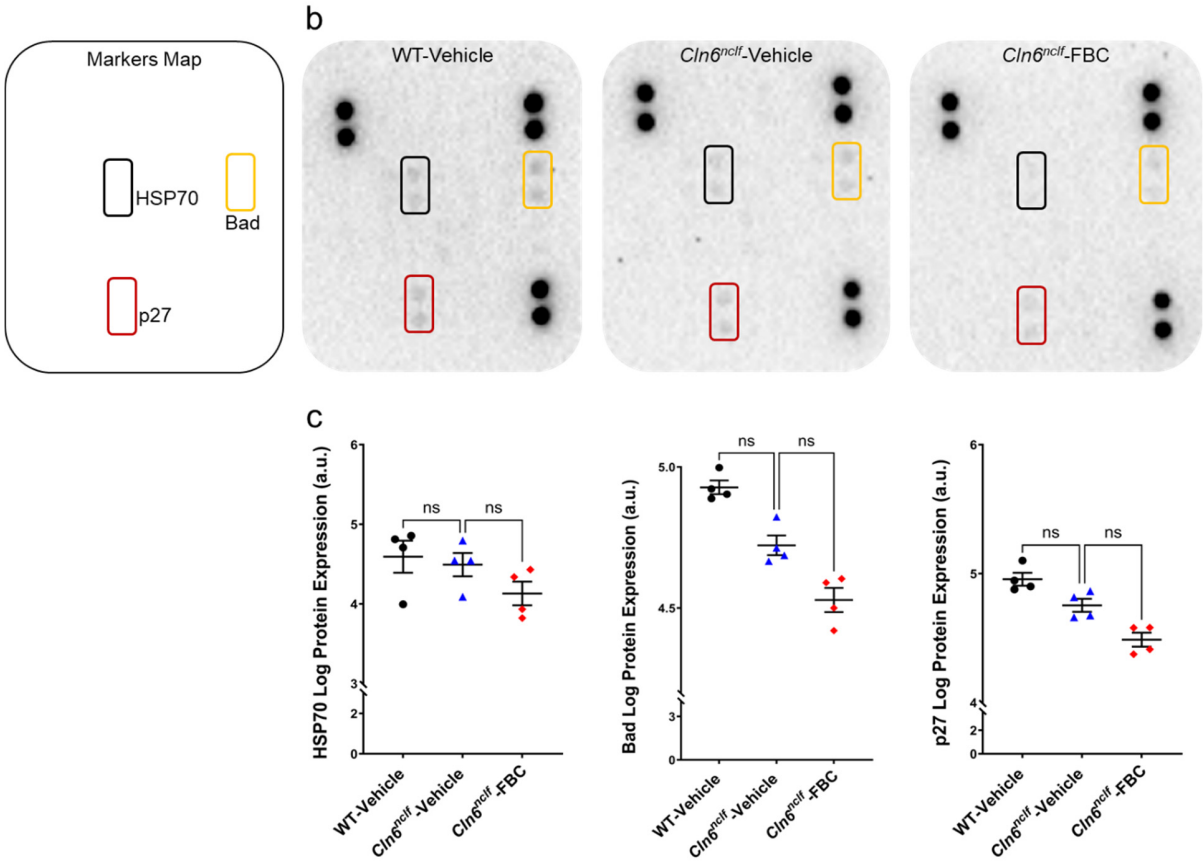
A Flupirtine Benzyl Carbamate Improves Neurocognitive Deficits and Molecular Pathology in the *Cln6*^{nclf} Mouse

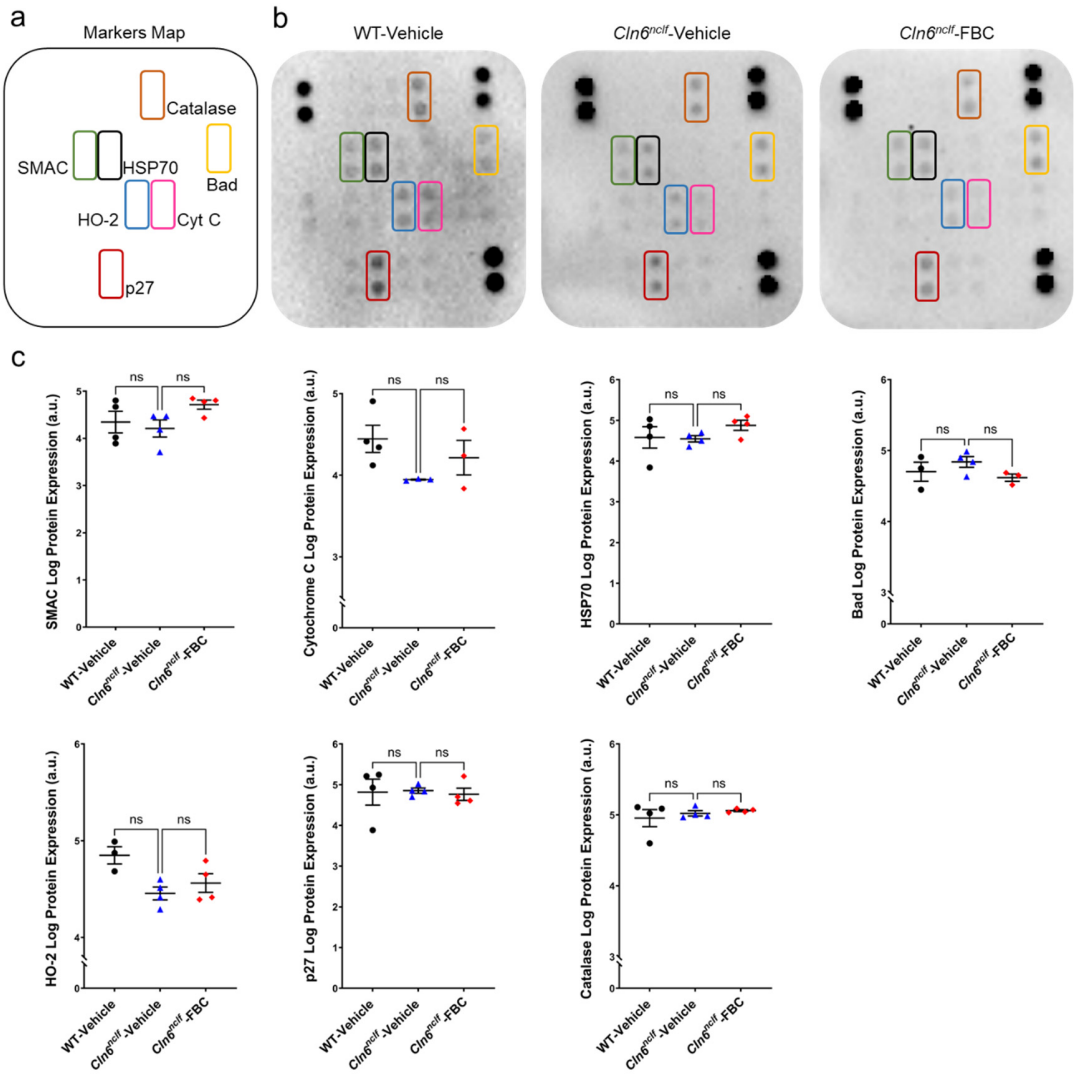
Victoria Chaoul [1], Omar Shmoury [1], Ramy Alam [1], Sara Saab [1], Joelle Makoukji [1,2], Lynn Al Aridi [1], Nadine J. Makhoul [1], Jihane Soueid [3], Angelica V. Carmona [4], Princess Simeon [4], Paul C. Trippier [4] and Rose-Mary Boustany [1,5,*]

[1] Department of Biochemistry and Molecular Genetics, American University of Beirut Medical Center, Riad El Solh, Beirut 1107 2020, Lebanon; vc07@aub.edu.lb (V.C.); sarasaab961@gmail.com (S.S.); lra16@mail.aub.edu (L.A.A.)
[2] Faculty of Health Sciences, Higher Colleges of Technology, Sharjah Campus A, P.O. Box 7946, Sharjah, United Arab Emirates
[3] Department of Anatomy, Cell Biology and Physiological Sciences, American University of Beirut,
Beirut 1107 2020, Lebanon
[4] Fred and Pamela Buffett Cancer Center, UNMC Center for Drug Discovery, Department of Pharmaceutical Sciences, University of Nebraska Medical Center, Omaha, NE 68105, USA; psimeon@unmc.edu (P.S.)
[5] Neurogenetics Program, AUBMC Special Kids Clinic, Division of Pediatric Neurology, Department of Pediatrics and Adolescent Medicine, American University of Beirut Medical Center,
Riad El Solh, Beirut 1107 2020, Lebanon
* Correspondence: rb50@aub.edu.lb; Tel.: +961-1-350000 (ext. 5640)

Supplementary Data

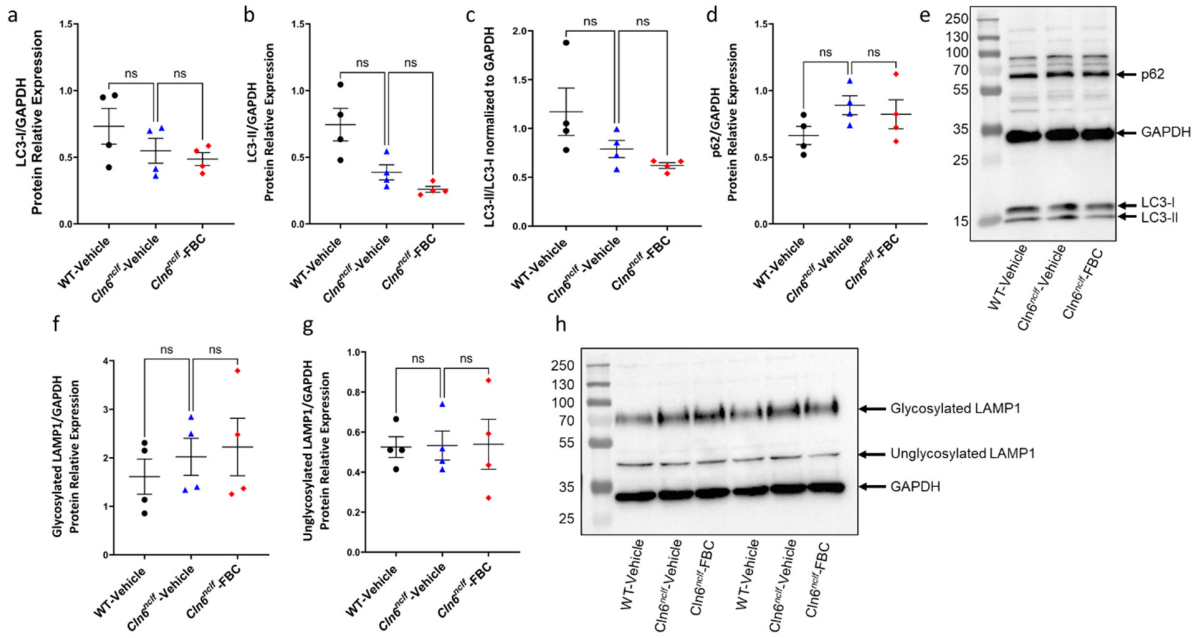


Supplementary Figure S1. Profiling of apoptosis-related protein markers in brains of male mice. (a) Schematic map of detected apoptosis-related markers. (b) Apoptosis proteome profiler dot blot arrays showing duplicates of three positive controls (at the corners) and of HSP70 (black), Bad (yellow) and p27 (red) in whole-brain lysates of WT vehicle-, *Cln6*^{nclf} vehicle- and *Cln6*^{nclf} FBC-treated male mice. (c) Dot plots illustrating the quantification by densitometry of HSP70, Bad and p27 protein expression from their respective dot blots (n=4/group). Statistical significance was determined via Kruskal–Wallis test followed by Dunn's post hoc multiple-comparisons test and data are presented as mean ± SEM. ns: not significant. HSP70: Heat shock protein 70, Bad: BCL-2-associated death promoter, p27: Cyclin-Dependent Kinase Inhibitor 1B.

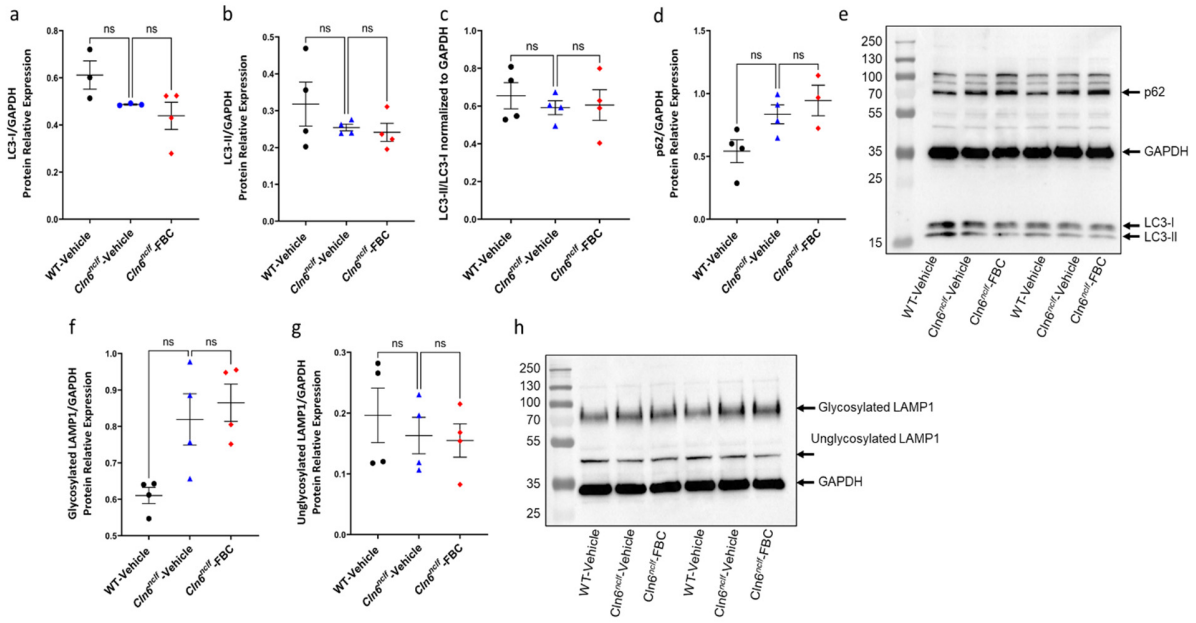


Supplementary Figure S2. Profiling of apoptosis-related protein markers in brains of female mice. (a) Schematic map of detected apoptosis-related markers. (b) Apoptosis proteome profiler dot blot arrays showing duplicates of three positive controls (at the corners) and of Catalase (Brown), SMAC (Green), HSP70 (Black), Bad (Yellow), HO-2 (Blue), Cyt C (Pink) and p27 (Red) in whole-brain lysates of WT vehicle-treated, *Cln6*^{nclf} vehicle-treated and *Cln6*^{nclf} FBC-treated female mice. (c) Dot plots illustrating the quantification by densitometry of Catalase, SMAC, HSP70, Bad, HO-2, Cyt C and p27 proteins from their respective dot blots (n=3–4/group). Statistical significance was determined via Kruskal–Wallis test followed by Dunn's post hoc multiple-comparisons test and data are presented as mean ± SEM. ns: not significant. SMAC: Second Mitochondria-derived Activator of Caspases, HSP70: Heat shock protein 70, Bad: BCL-2-associated death promoter, HO-2: Heme oxygenase-2, Cyt C: Cytochrome C, p27: Cyclin-Dependent Kinase Inhibitor 1B.

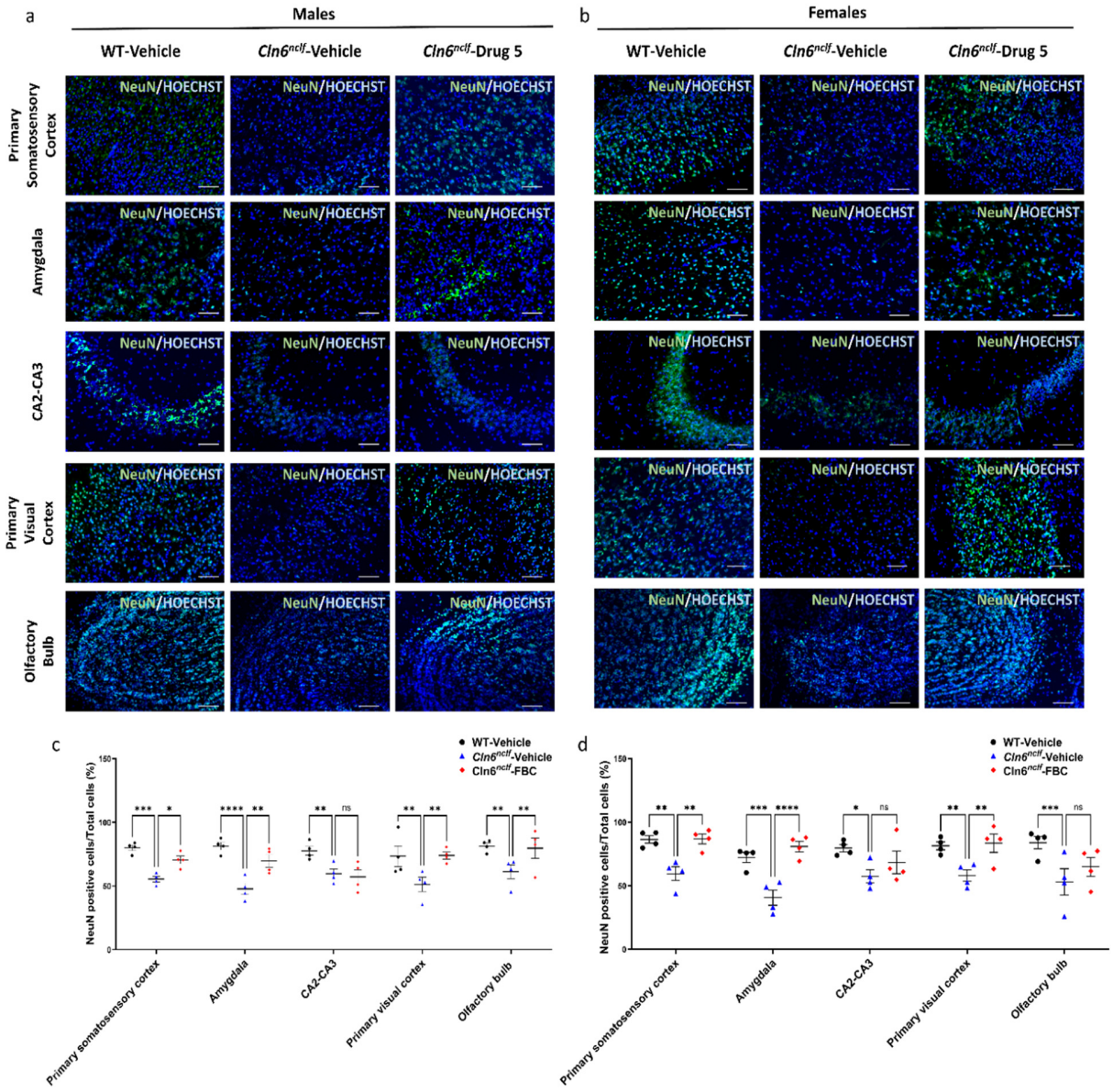
Western blot analysis of autophagy/lysosomal markers, microtubule-associated protein 1A/1B-light chain 3-I and II (LC3-I, LC3-II), p62/Sequestosome-1 (SQSTM1) and glycosylated/unglycosylated Lysosome-associated membrane protein 1 (LAMP1), was performed on brain lysates from WT vehicle-treated, *Cln6*^{nclf} vehicle-treated and *Cln6*^{nclf} FBC-treated male and female mice. Results are provided in Figure S3 & S4. Briefly, LC3-I, LC3-II and LC3-II/LC3-I ratio trended non-significantly lower in *Cln6*^{nclf} vehicle-treated vs WT vehicle-treated in both sexes and were not restored by FBC. p62, glycosylated and unglycosylated LAMP1 were unchanged in males and females across the three groups.



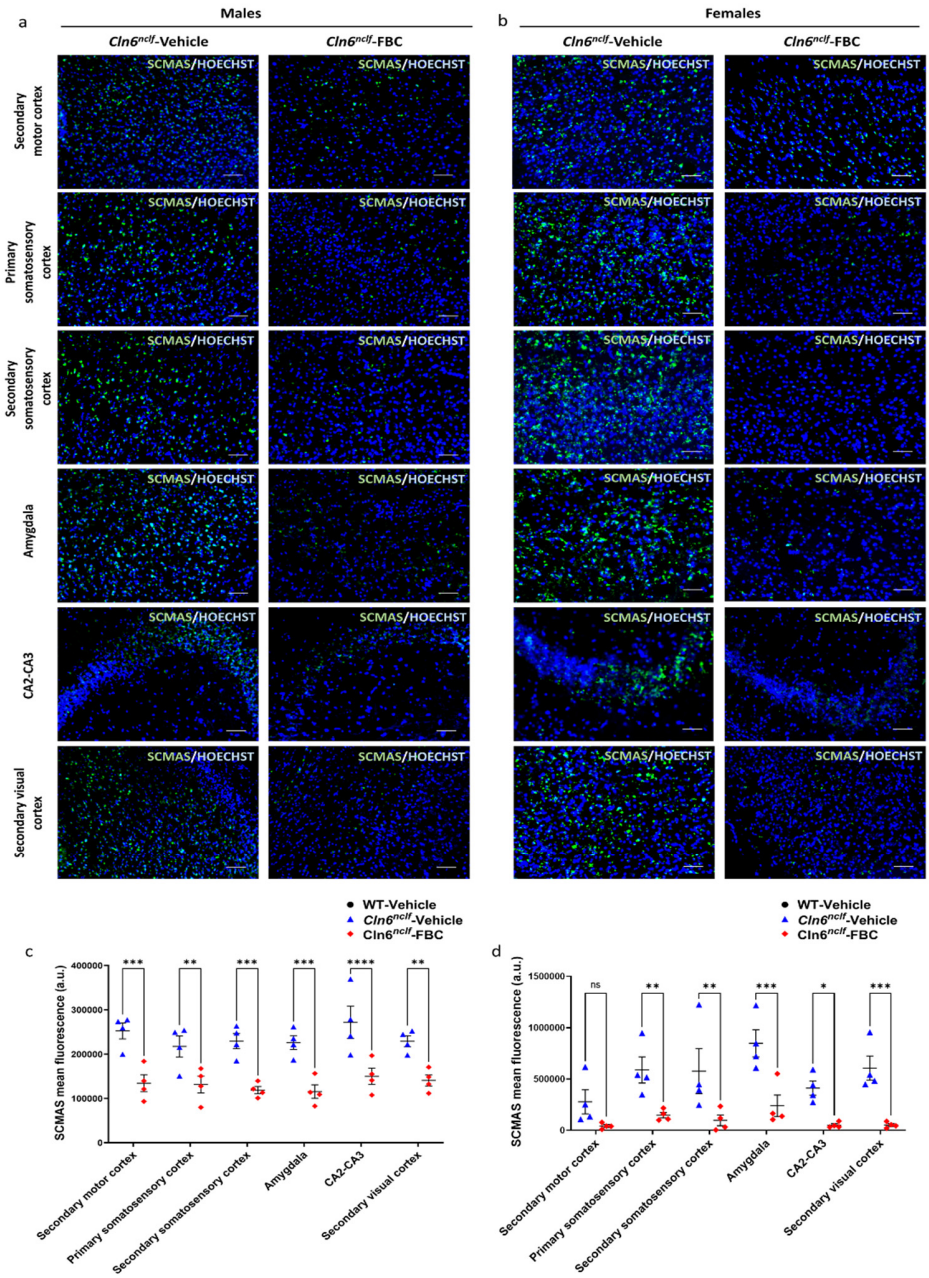
Supplementary Figure S3. Autophagy markers protein expression levels in brains of male mice. Dot plots representing the quantification by densitometry of autophagy-related proteins: (a) LC3-I, (b) LC3-II, (c) LC3-II/LC3-I ratio, (d) p62, (f) glycosylated LAMP1 and (g) unglycosylated LAMP1. Western blots (e, h) performed on whole-brain lysates from WT vehicle-treated, *Cln6*^{nclf} vehicle-treated, and *Cln6*^{nclf} FBC-treated male mice (n=4/group). All protein band intensities were normalized to GAPDH from their respective membranes. Statistical significance was determined via Kruskal–Wallis test followed by Dunn's post hoc multiple-comparisons test and data are represented as mean ± SEM. ns: not significant.



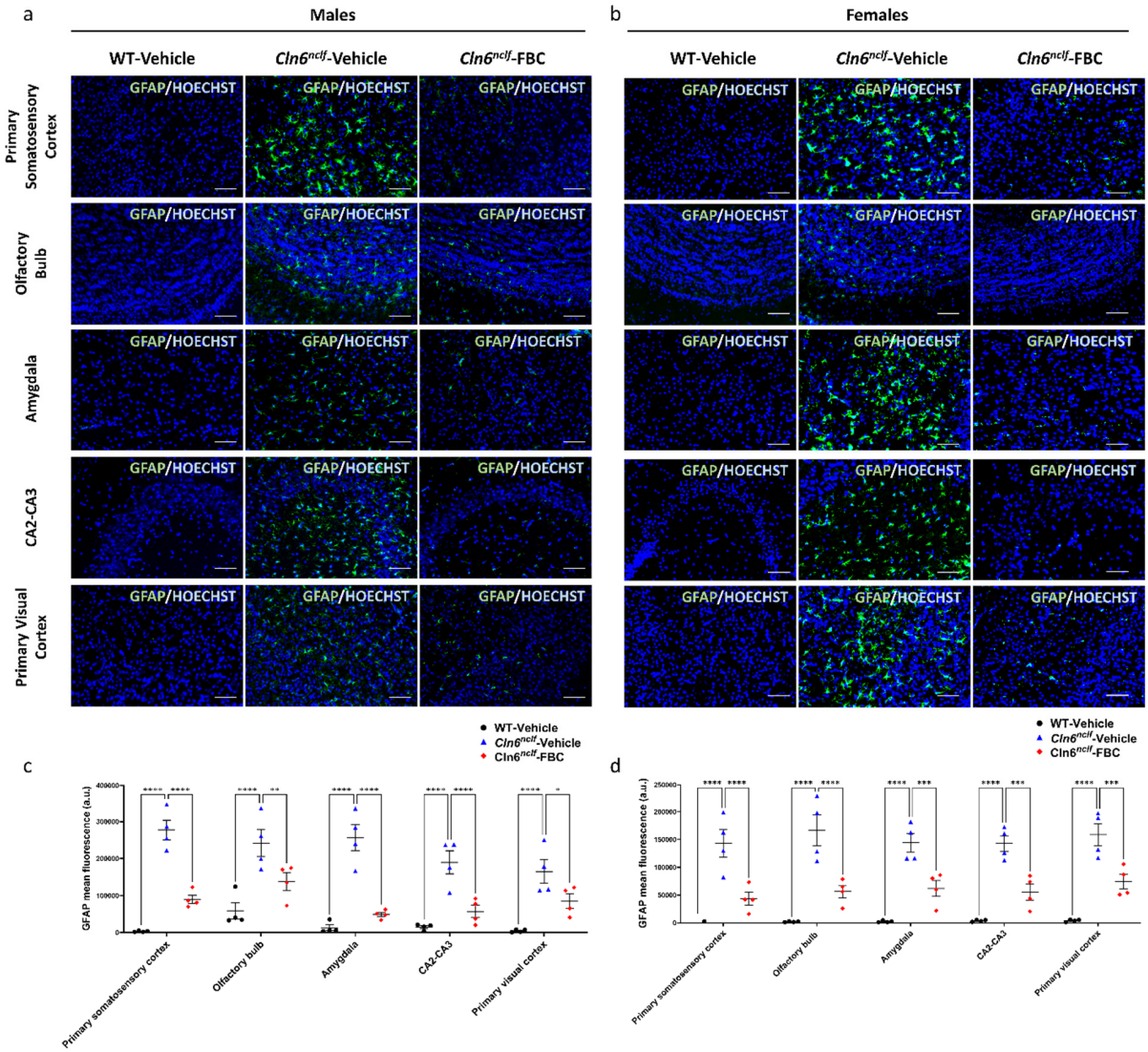
Supplementary Figure S4. Autophagy markers protein expression levels in brains of female mice. Dot plots representing the quantification by densitometry of autophagy-related proteins: (a) LC3-I, (b) LC3-II, (c) LC3-II/LC3-I ratio, (d) p62, (f) glycosylated LAMP1 and (g) unglycosylated LAMP1. Western blots (e, h) performed on whole-brain lysates from WT vehicle-treated, *Cln6*^{nclf} vehicle-treated, and *Cln6*^{nclf} FBC-treated female mice (n=3–4/group). All protein band intensities were normalized to GAPDH from their respective membranes. Statistical significance was determined via Kruskal–Wallis test followed by Dunn's post hoc multiple-comparisons test and data are represented as mean ± SEM. ns: not significant.



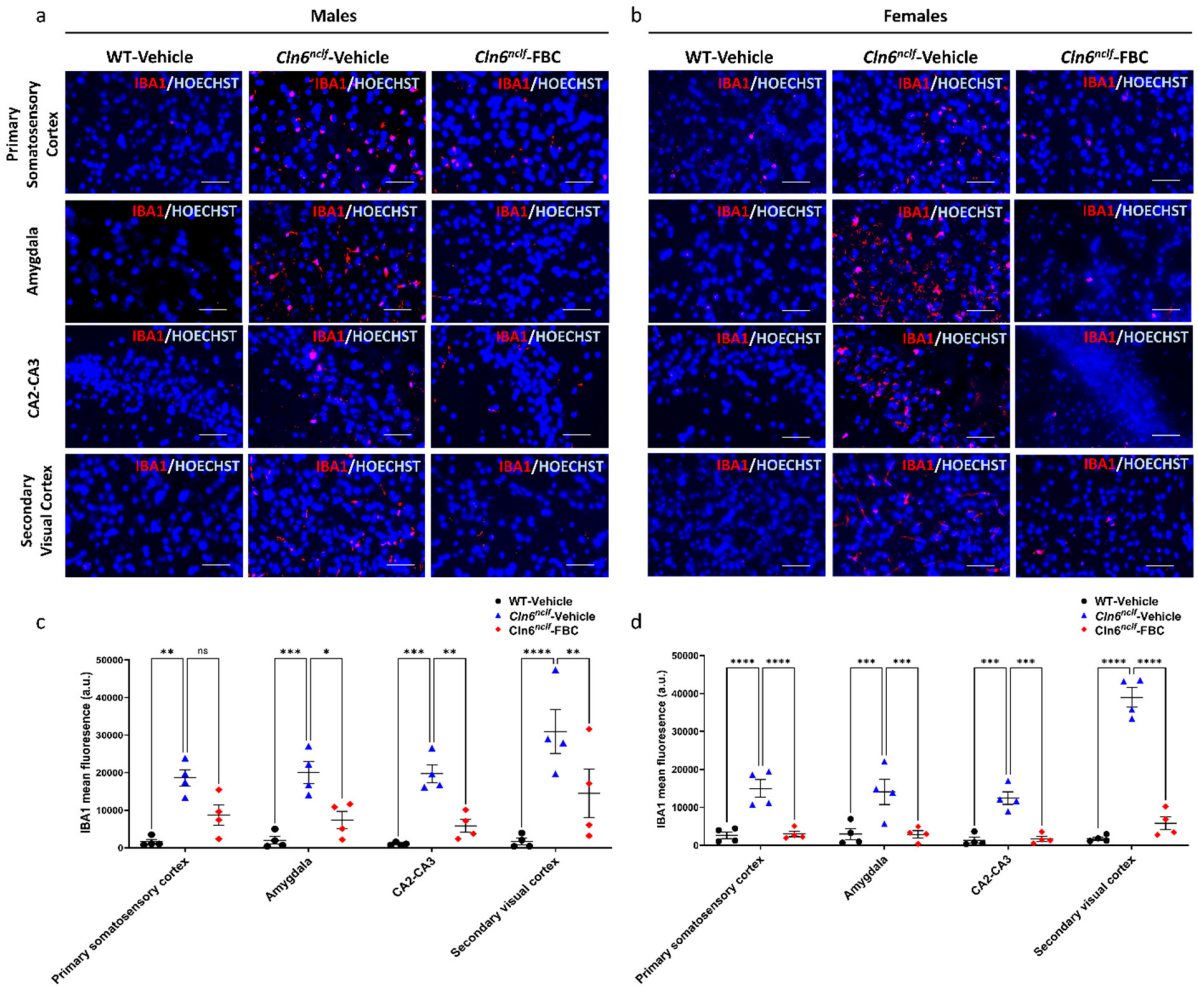
Supplementary Figure S5. Neuronal nuclei immunoreactivity in brains of male and female *Cln6*^{nclf} mice treated with FBC. Representative images of NeuN (green) immunofluorescence with Hoechst nuclear counterstain (blue) in coronal brain sections from 28-week-old male (a) and female (b) WT vehicle- (black circles), *Cln6*^{nclf} vehicle- (blue triangles) and *Cln6*^{nclf} FBC-treated mice (red diamonds). Images represent primary somatosensory cortex, amygdala, CA2-CA3, primary visual cortex and olfactory bulb. Scale bars: 100µm. Quantification of NeuN-positive cells divided by total number of cells in indicated regions in male (c) and female (d) mice. Each symbol represents an individual animal (n = 4 per group). Data are dis-played as mean ± SEM. Statistical comparisons were performed using two-way ANOVA followed by Fisher's LSD post hoc test. *p < 0.05, **p < 0.01, ***p < 0.001, ****p < 0.0001. ns: not significant.



Supplementary Figure S6. Accumulation of SCMAS in brains of male and female *Cln6*^{nclf} mice. Immunofluorescence images show SCMAS accumulation (green) in cells counterstained with Hoechst (blue) in coronal brain sections of 28-week-old male (a) and female (b) *Cln6*^{nclf} vehicle- (blue triangles) and *Cln6*^{nclf} FBC-treated (red diamonds) mice. Regions examined include secondary motor and visual cortices, primary/secondary somatosensory cortex, amygdala and CA2-CA3. Scale bars: 100µm. Dot plots summarizing SCMAS mean fluorescence intensity in brain regions of 28-week-old *Cln6*^{nclf} vehicle- and *Cln6*^{nclf} FBC-treated male (c) and female (d) mice. Each symbol represents an individual animal (n = 4 per group). Data are displayed as mean ± SEM. Statistical comparisons were performed using two-way ANOVA followed by Fisher's post hoc test. *p < 0.05, **p < 0.01, ***p < 0.001, ****p < 0.0001. ns: not significant.



Supplementary Figure S7. Astrogliosis in *Cln6*^{nclf} male and female mouse brain after treatment with FBC. Immunofluorescence images of 28-week-old male (a) and (b) female WT vehicle- (black circles), *Cln6*^{nclf} vehicle- (blue triangles) and *Cln6*^{nclf} FBC-treated (red diamonds) mouse brains confirm GFAP (green) with nuclear counterstain (Hoechst, blue) in primary somatosensory and visual cortices, olfactory bulb, amygdala and CA2-CA3. Scale bars: 100µm. Dot plots depict GFAP mean fluorescence intensity for brain areas for (c) males and (d) females. Each symbol represents an individual animal (n = 4 per group). Data are displayed as mean ± SEM. Statistical comparisons were performed using two-way ANOVA followed by Fisher's LSD post hoc test. *p < 0.05, **p < 0.01, ***p < 0.001, ****p < 0.0001.



Supplementary Figure S8. Microgliosis in *Cln6*^{nclf} male and female mouse brain treated with flupirtine benzyl carbamate. Immunofluorescence images of 28-week-old WT vehicle- (black circles), *Cln6*^{nclf} vehicle- (blue triangles) and *Cln6*^{nclf} FBC-treated (red diamonds) male (a) and female (b) mouse brain sections stained with IBA1 (red) and nuclear counterstain (Hoechst, blue) in primary somatosensory cortex, amygdala, CA2-CA3 and secondary visual cortex. Scale bars: 50µm. Dot plots depicting IBA1 mean fluorescence intensity for each brain area for (c) males and (d) females, with each symbol representing individual animal (n = 4 per group). Data are displayed as mean ± SEM. Statistical comparisons were performed using two-way ANOVA followed by Fisher's LSD post hoc test. *p < 0.05, **p < 0.01, ***p < 0.001, ****p < 0.0001. ns: not significant.